The functional importance of structural differences between the mannitol-specific IIAmannitol and the regulatory IIAnitrogen

Montfort, Rob L.M. van; Dijkstra, Bauke W.

Published in:
Protein Science

DOI:
10.1002/pro.5560071019

Protein Science (1998), 7:2210–2216. Cambridge University Press. Printed in the USA.

The functional importance of structural differences between the mannitol-specific IIA^{mannitol} and the regulatory IIA^{nitrogen}

ROB L.M. VAN MONTFORT AND BAUKE W. DIJKSTRA

Laboratory of Biophysical Chemistry and BIOSON Research Institute, University of Groningen, Nijenborgh 4, 9747 AG Groningen, The Netherlands

(RECEIVED April 1, 1998; ACCEPTED July 1, 1998)

Abstract

The three-dimensional structures of the IIA domain of the mannitol-specific phosphoenol-pyruvate dependent phosphotransferase system (PTS) of *Escherichia coli* and the regulatory IIA^{ntr} enzyme have been compared. The enzymes are 20% identical in sequence and contain the sequence motif specific for IIA proteins belonging to the mannitol-fructose family of the PTS. The fold of the enzymes is nearly identical, which confirms their evolution from a common ancestor. Moreover, the phosphorylation site of IIA^{mtl} (His65) and one of the observed conformations of the active site Arg49 are extremely similar to their equivalents (His73 and Arg57) in IIA^{ntr}. In contrast, His120, the equivalent of the second active site His111 of IIA^{mtl}, is not located in the active site of IIA^{ntr} but points into the solvent on the other side of the molecule. The different position of His120 makes it unlikely that this residue assists in phosphoryl transfer in the regulatory IIA^{ntr}s. As His120 is conserved in all IIA^{ntr} enzymes, it could have an essential role in the recognition of the target protein of IIA^{ntr}.

Keywords: carbohydrate transport; IIA domains; nitrogen metabolism; PTS; sigma 54; X-ray structure

With the massive amounts of sequence data becoming available through the genome sequencing projects, we are challenged to link the many newly discovered genes to the function of their protein products. An important tool to get insight in the function of these novel proteins is the comparison of their amino acid sequences with sequences of proteins with known function or activity (Friedrich, 1996). However, even if significant sequence similarity is present, proteins can have very different functions. An example are the proteins homologous to the IIA enzymes of the mannitol-fructose family of the bacterial phosphoenolpyruvate-dependent phosphotransferase system (PTS).

The PTS catalyzes the uptake of carbohydrates and their concurrent phosphorylation (Postma et al., 1993; Lengeler et al., 1994). In addition, the PTS plays a crucial role in the global regulation of the cellular metabolism (Saier & Reizer, 1994), and in chemotaxis toward PTS-substrates (Lux et al., 1995). It is composed of three catalytic entities, the general proteins enzyme I (E_I), the histidine-containing protein (HPr), and the carbohydrate-specific enzyme II complex (E_{II}). Energy to drive the translocation of the carbohydrate is provided by phosphoenol-pyruvate (PEP). A phosphoryl group is abstracted from PEP by E_I, and via HPr, transferred to E_{II}. E_{II}s are usually composed of at least three functional domains, two cytoplasmic domains, IIA and IIB, and the transmembrane channel IIC. HPr phosphorylates IIA, which, in turn, transfers the phosphoryl group to IIB. The phosphorylated state of IIB triggers efficient transport by IIC and subsequently phosphorylates the transported carbohydrate (Lolkema et al., 1991). In the different E_{II}s these domains may be linked in different ways. For example, in the mannitol-specific E_{II} from *Escherichia coli* the domains are present on a single polypeptide chain (Lee & Saier, 1983), whereas the mannitol-specific E_{II} from *Bacillus stearothermophilus* is composed of a separate IIA domain and a linked IIB and IIC (Henstra et al., 1996).

Several Gram-negative bacteria possess a IIA-homologue that is cotranscribed with, and negatively regulates, sigma factor σ54 (Reizer et al., 1992; Begley & Jacobson, 1994; Powell et al., 1995; Du et al., 1996). The novel IIA proteins have been named IIA^{ntr} (nitrogen related IIA), because in *E. coli* σ54 is a key sigma factor in the transcription of genes involved in nitrogen metabolism. IIA^{ntr} can be phosphorylated by HPr, or by the HPr-homologue NPr (nitrogen related HPr), which is also cotranscribed with σ54 (Begley & Jacobson, 1994; Powell et al., 1995). These observations led to the proposal that IIA^{ntr} might provide a regulatory link between the PTS and nitrogen metabolism in bacteria (Reizer et al., 1992). But, since not all σ54-dependent operons are involved in nitrogen metabolism, IIA^{ntr} may be part of a sensory

Reprint request to: B.W. Dijkstra, Laboratory of Biophysical Chemistry, University of Groningen, Nijenborgh 4, 9747 AG Groningen, The Netherlands; e-mail: bauke@chem.rug.nl.

system that monitors the energy status of the cell and modulates σ54-dependent transcription accordingly (Merrick, 1993; Merrick et al., 1995).

Reizer et al. proposed a sequence motif (see Fig. 1) for IIA enzymes of the mannitol-fructose family consisting of the active site histidine and several other functionally essential residues (Reizer et al., 1992). The motif is present in IIA^{ntr} proteins as well, suggesting that the sugar transport IIA proteins and the regulatory IIA^{ntr} enzymes could have evolved from a common ancestor. Recently, we reported the structure determination of the IIA domain of the mannitol transporter of *E. coli*, IIA^{mtl} (van Montfort et al., 1998) and of *E. coli* IIA^{ntr} (Bordo et al., 1998). The proteins share approximately 20% sequence identity. In this article we present a detailed comparison of the structures of IIA^{mtl} and IIA^{ntr}. Our results show that subtle differences in three-dimensional structure may give rise to considerable differences in functionality.

Materials and methods

The structure of the IIA^{mtl} domain of *E. coli* was solved by X-ray crystallography to 1.8 Å resolution with an *R*-factor of 19.0% (R_{free} 24.2%) (van Montfort et al., 1998). The protein model of IIA^{mtl} (PDB entry 1a3a) contains four independent molecules, which are related by noncrystallographic symmetry. The four molecules form two dimers. Dimer A is composed of molecules IIA$^{mtl_{AI}}$ and IIA$^{mtl_{AII}}$, and dimer B is composed of molecules IIA$^{mtl_{BI}}$ and IIA$^{mtl_{BII}}$. Although the overall structures of the four molecules are identical, two different conformations of IIA^{mtl} are observed. One conformation is represented by molecules IIA$^{mtl_{AI}}$ and IIA$^{mtl_{BI}}$, the other by IIA$^{mtl_{AII}}$ and IIA$^{mtl_{BII}}$. The differences between the two IIA^{mtl} conformations are mainly located in regions on the surface of the protein, which are involved in contacts with neighboring molecules, and in the active site.

The structure of IIA^{ntr} was solved to 2.35 Å with an *R*-factor of 19.5% (R_{free} 25.1%) (Bordo et al., 1998). The IIA^{ntr} model (PDB entry 1a6j) contains two independent molecules, IIA^{ntr_A} and IIA^{ntr_B}. The first seven residues in IIA^{ntr_A} are disordered. The corresponding residues in molecule IIA^{ntr_B} bind in the active site of molecule IIA^{ntr_A}, which most likely causes their well-defined conformation. The first three residues adopt an extended conformation, while residues 4 to 10 form a short α-helix. As in IIA^{mtl}, the main differences between the two independent molecules occur in regions that interact with molecules related by crystallographic and noncrystallographic symmetry. For the comparison of IIA^{mtl} and IIA^{ntr}, we selected molecule IIA$^{mtl_{AI}}$ and IIA$^{mtl_{AII}}$, which represent the two observed IIA^{mtl} conformations, and molecule IIA^{ntr_B} to represent the IIA^{ntr} structure. The secondary structure was assigned using the method of Kabsch and Sander (1983), implemented in the program PROCHECK (Laskowski et al., 1993). The superimpositions of IIA^{ntr_B} on IIA$^{mtl_{AI}}$ and IIA$^{mtl_{AII}}$ were carried out with the least-squares structure comparison routine in O (Jones et al., 1991), and manually inspected for their accuracy. The best match between their phosphorylation sites and central β-sheets has been obtained using the Cα-atoms of residues 19 to 22, 63 to 74, 85 to 90, and 105 to 110 of IIA^{ntr_B}, and 12 to 15, 55 to 66, 79 to 84, and 99 to 104 of the IIA^{mtl} molecules. The respective superimpositions yielded RMS fit values of 0.65 Å and 0.72 Å for 28 equivalent Cα-pairs.

Results and discussion

Structure-based sequence comparison

With 148 amino acids (M_r 16.3 kDa), IIA^{mtl} is somewhat smaller than IIA^{ntr}, which contains 163 amino acids (M_r 17.9 kDa). A structure-based sequence comparison (Fig. 1) shows that this difference in size is mostly due to extensions at the N- and C-termini

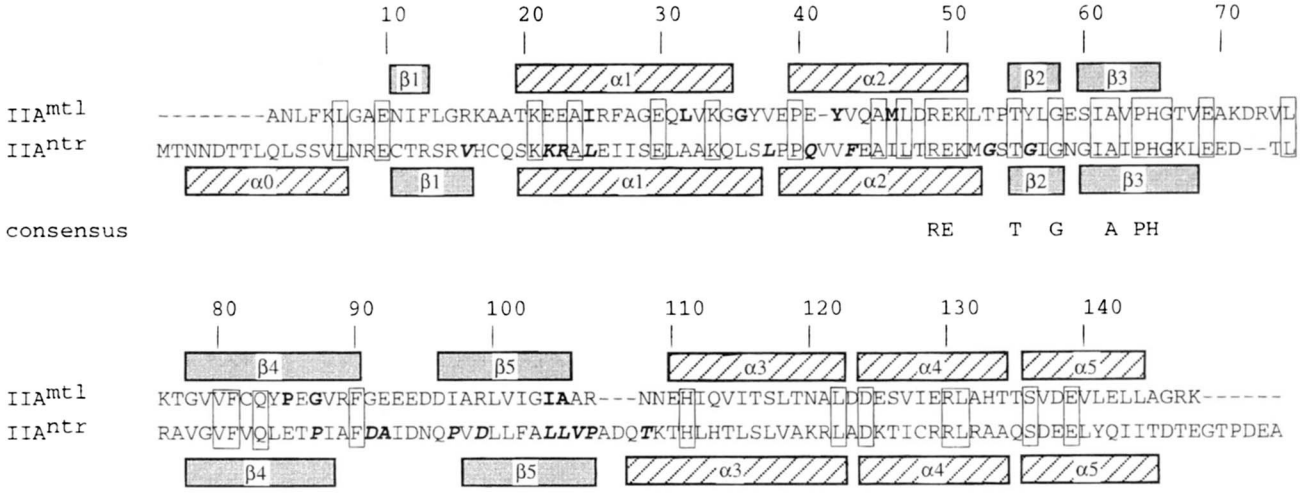

Fig. 1. Structure-based sequence alignment of *E. coli* IIA^{mtl} and IIA^{ntr}. The amino acid numbering is that of IIA^{mtl}. Secondary structure assignments are shown for both proteins; strands are shown in grey; helices are shaded. Gaps in the alignment are indicated with a dash. Residues conserved between IIA^{mtl} and IIA^{ntr} are boxed, the residues specific for the IIA^{mtl} and IIA^{fru} proteins are shown in bold, and the residues specific for IIA^{ntr} are shown in bold italic. The assignment is based on a sequence comparison comprising the IIA^{mtl} domains from *E. coli* (Lee & Saier, 1983), *B. stearothermophilus* (Henstra et al., 1996), *Bacillus subtilis* (Akagawa et al., 1995), *Enterococcus faecalis* (Fischer et al., 1991), *Staphylococcus carnosus* (Fischer et al., 1989) and *Streptococcus mutans* (Honeyman & Curtiss, 1992), the IIA^{fru} proteins from *E. coli* (Reizer et al., 1994), *Haemophilus influenza* (Fleischmann et al., 1995), *Salmonella typhimurium* (Geerse et al., 1989), *Rhodobacter capsulatus* (Wu et al., 1990), and *Xanthomonas campestris* (de Crécy-Lagard et al., 1995), and the sequences of IIA^{ntr} from *E. coli* (Powell et al., 1995), *Klebsiella pneumonia* (Merrick & Coppard, 1989), *Pseudomonas putida* (Inouye et al., 1989), and *H. influenza* (Fleischmann et al., 1995).

of IIA^{ntr}. However, the truncation of IIA^{mtl} at the N-terminus is caused by the subcloning procedure (van Weeghel et al., 1991): in the intact E_{II}^{mtl} the IIA^{mtl} domain is covalently connected to IIB^{mtl} via an N-terminal flexible linker. Neither seems the difference at the C-terminus of structural significance, since the last six residues of IIA^{ntr} are not visible in the electron density suggesting that they are flexible.

The sequence identity of IIA^{mtl} and IIA^{ntr} from *E. coli*, calculated from the structure-based sequence comparison, is approximately 20% (Fig. 1). Both proteins contain the sequence motif, specific for IIA domains of the mannitol-fructose enzyme II family. This suggests that they are evolutionary related. However, as will be outlined below, the X-ray structures show some significant differences, which are most likely related to their different functions in the bacterial cell.

The X-ray structures of IIA^{mtl} and IIA^{ntr}

The structure of IIA^{mtl} consists of a central five-stranded mixed β-sheet, flanked by α-helices on either side of the sheet (Fig. 2A). The β-sheet is composed of two pairs of parallel β-strands oriented antiparallel to each other, flanked by a short fifth strand of two residues. The order of the β-strands is 14532. Two α-helices pack on one side of the sheet, three are located on the other side. The phosphorylation site His65 is located in a shallow crevice at the surface of the protein.

The core of IIA^{ntr} has roughly the same size as IIA^{mtl} and its fold is very similar (Fig. 2B). It also consists of a central 5-stranded mixed β-sheet, packed with α-helices on both sides, and the active site is located in an equivalent position. Molecule IIA^{ntr_B} possesses an extra N-terminal α-helix (α0). However, since this helix blocks the active site of IIA^{ntr_A}, and the N-terminal residues of IIA^{ntr_A} are disordered, its functional importance is doubtful, and its secondary structure might be a consequence of crystal packing.

A superimposition of IIA^{mtl} and IIA^{ntr} reveals significant differences in and near their active sites. While the upper parts of the β-sheets (Fig. 2) superimpose closely, the strands diverge in the parts close to the respective phosphorylation sites, His65 in IIA^{mtl} and His73 in IIA^{ntr} (Fig. 3). The β-strands containing the histidine phosphorylation sites (β-strands β3) show the largest difference. In IIA^{mtl}, the catalytic histidine marks the end of the β-strand, whereas in IIA^{ntr} the strand extends three residues beyond the phosphorylation site. The three extra residues of the β3 strand in IIA^{ntr} form a regular β-sheet hydrogen bonding pattern with the C-terminal end of the neighboring strand β5, which is two residues longer than the corresponding strand in IIA^{mtl}. In this way the β3 strand in IIA^{ntr} is firmly attached to the rest of the structure and provides a solid foundation for the phosphorylation site.

In contrast, in IIA^{mtl} the C-terminal end of the β3 strand is anchored to the neighboring β5 strand via hydrogen bonds of the hydroxyl group of Tyr42 to the backbone amide group of Gly66, and the carbonyl oxygen atom of Ala105. The side chain of Tyr42 is also part of a hydrophobic cluster, which further stabilizes this part of the structure. Like Met46, another residue in the hydrophobic cluster, Tyr42 is conserved in all mannitol/fructose-specific IIA proteins. In the IIA^{ntr} enzymes, the equivalent of Tyr42 is a valine or isoleucine. The valine side chain of *E. coli* IIA^{ntr} adopts a different position from Tyr42 of IIA^{mtl}, which may be attributed to its size, and to its inability to make hydrogen bonds.

In both enzymes the α-helices surrounding the central β-sheet are located in similar positions. However, the third α-helix in IIA^{ntr} (α3) is tilted by approximately 15° with respect to the corresponding α-helix in IIA^{mtl} (Fig. 3B). The tilt is probably induced by the longer β5 strand, an insertion of three residues in the loop between β5 and α3, and one additional turn of α3 at its N-terminal end. This tilt drastically affects the position of His120 with respect to the equivalent His111 in IIA^{mtl}, and has significant functional implications (see below).

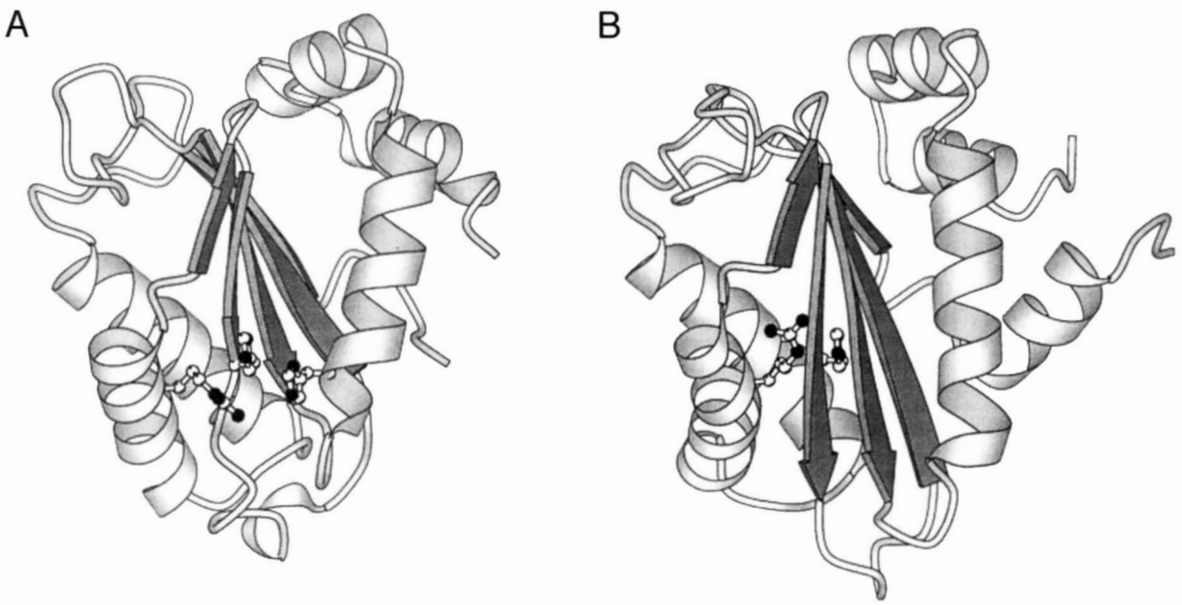

Fig. 2. Comparison of the structures of (**A**) IIA^{mtl} and (**B**) IIA^{ntr}. The catalytic histidines are shown in ball and stick representation.

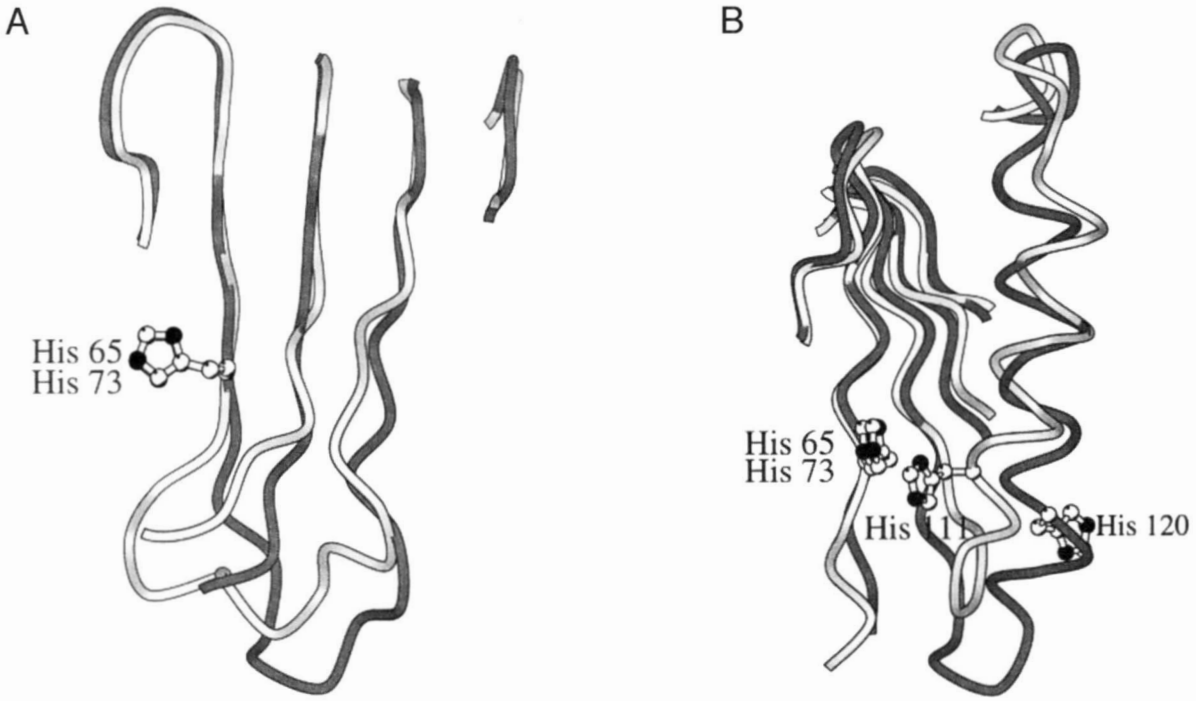

Fig. 3. A: Superposition of the central β-sheets of IIA^{mtl} in light grey and IIA^{ntr} in dark grey. The phosphorylation sites, His65 in IIA^{mtl} and His73 in IIA^{ntr}, are shown in a ball and stick representation. **B:** Superposition of the central β-sheets of IIA^{mtl} and IIA^{ntr} and the α-helices containing the second conserved histidine, His111 in IIA^{mtl} and His120 in IIA^{ntr}. The histidines are shown in ball and stick representation.

The phosphorylation site

The IIA^{mtl} phosphorylation site His65 is located at the end of the third β-strand and forms the center of a shallow crevice at the surface of the protein. The imidazole ring of His65 is kept in position by a hydrogen bond of its Nδ atom with the carbonyl oxygen of Val 63 (Fig. 4). This places the Nϵ atom of the histidine side chain in an excellent position to perform a nucleophilic attack on an incoming phosphoryl group. The IIA^{ntr} catalytic His73 is located in an equivalent position, and its side chain has a similar hydrogen bonding interaction but with the carbonyl oxygen of Ile71. The presence of this hydrogen bond explains the invariance of the proline residue before the phosphorylation site. The proline side chain is oriented almost perpendicular to the plane of the central β-sheet. As a consequence, the carbonyl group of the preceding residue (Val63 in IIA^{mtl}, Ile71 in IIA^{ntr}) is forced to be perpendicular to the sheet as well, in an eminently favourable position to form the hydrogen bond with the Nδ atom of the catalytic histidine (Fig. 4). In addition to its role in positioning the imidazole ring, the presence of the hydrogen bond might increase the nucleophilicity of the Nϵ atom of the catalytic histidine, a role also proposed for the hydrogen bond between the carbonyl oxygen of Gly92 and the Nδ of the catalytic histidine, His90, in *E. coli* glucose-specific IIA^{glc} (Pelton et al., 1996). The latter protein has a fold and amino acid sequence completely unrelated to those of IIA^{mtl} (van Montfort et al., 1998).

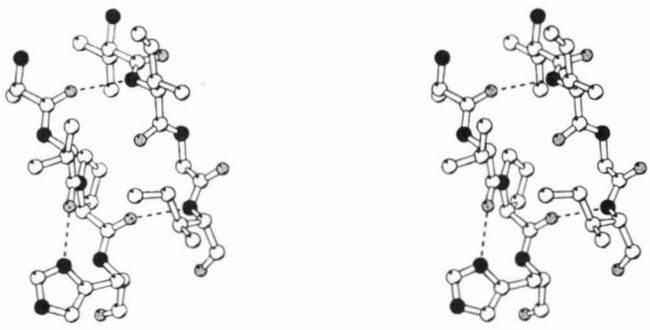

Fig. 4. Ball and stick representation of the third and fifth β-strand of IIA^{mtl}. Hydrogen bonds are shown as dashed lines.

The active site arginine

The arginine of the consensus motif (Arg49) adopts two conformations in the four independent IIA^{mtl} molecules (Fig. 5A). As IIA^{mtl} is involved in two phosphoryl transfer reactions, phosphorylation by HPr and dephosphorylation by IIB^{mtl}, it has been suggested that these two conformations might represent the states of the active site required for the different phosphoryl transfer reactions (van Montfort et al., 1998). In IIA^{mtl}$_{A1}$ the side chain of Arg49 points away from the phosphorylation site and therefore has an unfavorable conformation to stabilize the phosphorylated protein, or a transition state intermediate. However, this conformation might

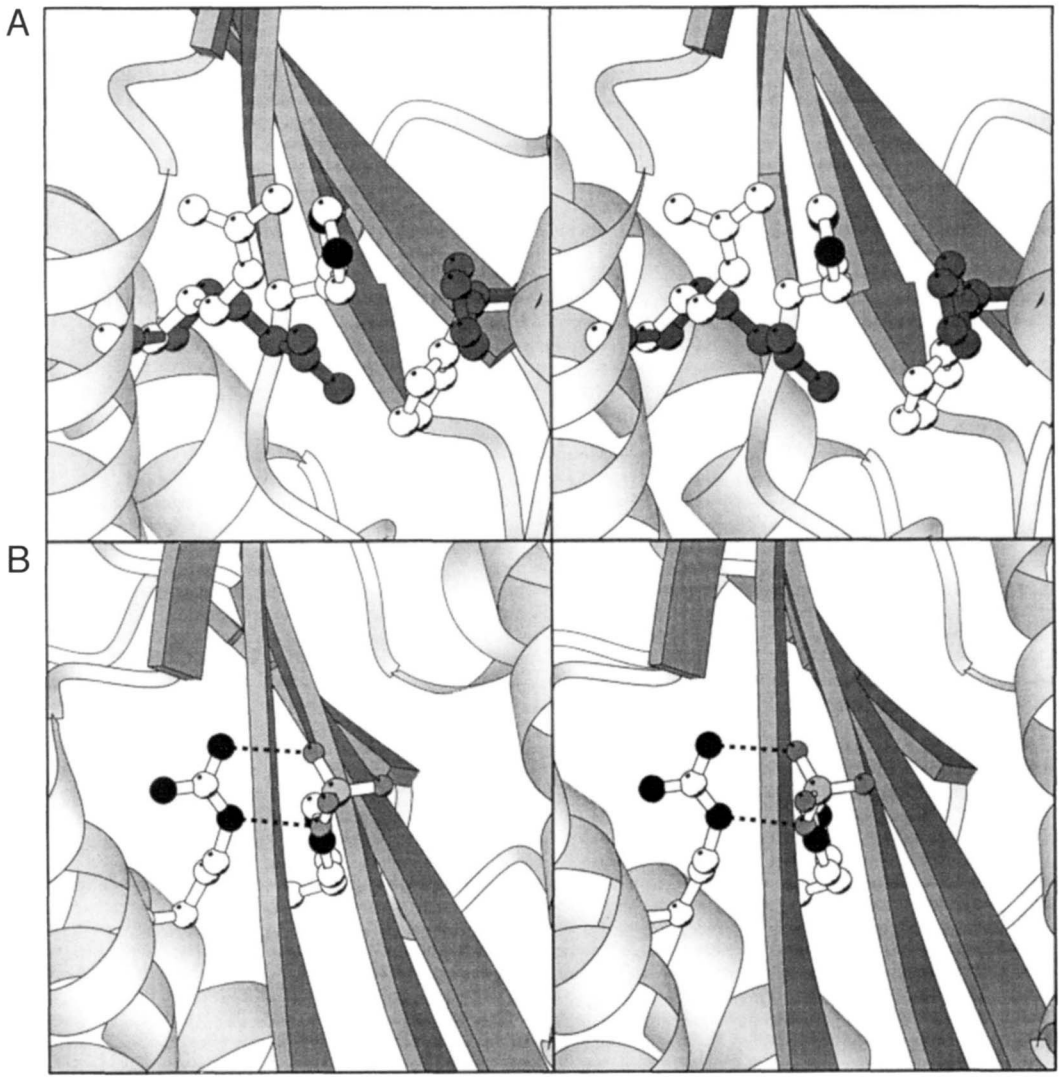

Fig. 5. A: Stereo figure of the active site of IIA^{mtl} showing the two conformations of Arg49 and His111 in dark grey and white, respectively. Also shown is the phosphorylation site His65. **B:** Stereo figure of the active site of IIA^{ntr_B}. The active site Arg57 and His73 are shown in ball and stick representation. Also shown is the bound sulfate ion.

be favorable in the dephosphorylation of His65 by IIB^{mtl}, in which phospho-IIA^{mtl} should not be stabilized.

In $IIA^{mtl_{AII}}$, the conformation of Arg49 resembles that of the equivalent Arg57 in IIA^{ntr} (Fig. 5B). In this conformation the guanidinium group is positioned close to the phosphorylation site in an excellent position to interact with the oxygen atoms of an incoming or covalently linked phosphoryl group, suggesting that it represents the conformation needed for phosphorylation by HPr or NPr. This notion is supported by the presence of a sulfate ion in the active site of IIA^{ntr_B}, hydrogen bonded to the Nϵ and Nη2 atoms of Arg57, which could mimic a bound phosphoryl group.

The second conserved histidine

The phosphorylation site His65 in IIA^{mtl} is flanked by the conserved His111, which has been proposed to be essential for the phosphoryl transfer from IIA^{mtl} to IIB^{mtl} (Reizer et al., 1992). Like Arg49, His111 adopts two conformations in the different IIA^{mtl} molecules (Fig. 5A) (van Montfort et al., 1998). In $IIA^{mtl_{AII}}$, where the side chain of Arg49 is close to the phosphorylation site, the imidazole ring of His111 points away, making a role in phosphoryl transfer to IIB^{mtl} unlikely. However, in molecule $IIA^{mtl_{AI}}$, where the Arg49 side chain points away from the phosphorylation site, the side chain of His111 is almost parallel to the side chain of His65. In this conformation His111 is likely to be closer to the phosphoryl group in a IIA^{mtl}-IIB^{mtl} complex, and thus could play a role in phosphoryl transfer to IIB^{mtl}.

His120 in IIA^{ntr} is equivalent to His111 in IIA^{mtl} but it does not superimpose at all with His111. Its side chain is not found in the active site, but points into the solvent on the other side of the molecule (Fig. 3). This difference in position is the result of the 15° tilt of the α3 helix of IIA^{ntr} described above. To bring His120 in IIA^{ntr} near the phosphorylation site would require a rotation or local unwinding of the N-terminal part of the helix. Hence, whereas

the position of His111 in IIA^{mtl} would allow its involvement in phosphoryl transfer from IIA^{mtl} to IIB^{mtl}, the present location of His120 in our IIA^{ntr} structure seems unlikely to allow this residue to play a direct role in the phosphoryl transfer from IIA^{ntr} to other proteins.

Conclusions

The similarity in fold of IIA^{mtl} and IIA^{ntr} supports the hypothesis that both proteins have evolved from a common ancestor, and confirms IIA^{ntr} as a member of the IIA proteins of the mannitol-fructose family. Characteristics of the IIA^{mtl}-fold are a five-stranded mixed β-sheet, flanked by α-helices. The phosphorylation site is located in a shallow groove at the surface of the protein.

Although the overall fold of the enzymes is nearly identical, pronounced structural differences exist in and near their active sites. These differences include a three residues elongation of β-strand β3 in IIA^{ntr} and the substitution of Tyr42 in IIA^{mtl} with a valine in IIA^{ntr}. The 15° tilt of α-helix α3 in IIA^{ntr}, probably as a result of two extra residues on the C-terminal end of β-strand β5, the insertion of three residues in the loop between β-strand β5 and α-helix α3, and the earlier start of helix α3, seem to be of major importance for the difference in function of the two proteins.

Phosphorylation of IIA^{mtl} and IIA^{ntr} by HPr, or the HPr homologue NPr, most likely proceeds via similar mechanisms. This is reflected by the identical positions and conformations of the respective phosphorylation sites and the conformations of the active site arginine residues in IIA^{ntr} and IIA^{mtl}$_{AII}$. In contrast, the difference in the position of the second conserved histidine (His111 in IIA^{mtl}, His120 in IIA^{ntr}) might reflect differences in the dephosphorylation reaction of both enzymes. Whereas IIA^{mtl} is dephosphorylated by IIB^{mtl}, in which reaction His111 is suggested to play an essential role (Reizer et al., 1992), no IIB^{ntr} has been found to date. Moreover, although IIA^{ntr} can be easily phosphorylated by HPr, it can not substitute for mannitol- or fructose-specific IIA proteins in PTS mediated transport of these carbohydrates (Powell et al., 1995). This suggests that IIA^{ntr} is not able to transfer a phosphoryl group to mannitol- or fructose-specific IIB domains. Hence, IIA^{ntr} might interact with proteins using a phosphorylation mechanism, which does not require the involvement of a second histidine, or perform its regulatory role by binding to other proteins in its phosphorylated or dephosphorylated state. In addition, the difference in position of the histidines might be part of a clever mechanism of the bacterium to prevent unwanted cross-talk between the regulatory tasks of IIA^{ntr} and PTS-dependent mannitol- or fructose-uptake.

Acknowledgments

We thank George Robillard for stimulating discussions during the preparation of this manuscript.

References

Akagawa E, Kurita K, Sugawara T, Nakamura K, Kasahara Y, Ogasawara N, Yamane K. 1995. Determination of a 17484 bp nucleotide sequence around the 39 degrees region of the *Bacillus subtilis* chromosome and similarity analysis of the products of putative ORFs. *Microbiology 141*:3241–3245.

Begley GS, Jacobson GR. 1994. Overexpression, phosphorylation, and growth effects of ORF162, a *Klebsiella pneumoniae* protein that is encoded by a gene linked to *rpoN*, the gene encoding σ^{54}. *FEMS Microbiol Lett 119*:389–394.

Bordo D, van Montfort RLM, Pijning T, Kalk KH, Reizer J, Dijkstra BW. 1998. The three-dimensional structure of the nitrogen regulatory bacterial protein IIA^{nitrogen}. *Mol Biol 279*:245–255.

de Crécy-Lagard V, Binet M, Danchin A. 1995. Fructose phosphotransferase system of *Xanthomonas campestris* pv. campestris: Characterisation of the *fruB* gene. *Microbiology 141*:2253–2260.

Du Y, Holtel A, Reizer J, Saier MH Jr. 1996. σ^{54}-dependent transcription of the *Pseudomonas putida xylS* operon is influenced by the IIA^{ntr} protein of the phosphotransferase system in *Escherichia coli*. *Res Microbiol 147*:129–132.

Fischer R, Eisermann R, Reiche B, Hengstenberg W. 1989. Cloning, sequencing and overexpression of the mannitol-specific enzyme-III-encoding gene of *Staphylococcus carnosus*. *Gene 82*:249–257.

Fischer R, von Strandmann R, Hengstenberg W. 1991. Mannitol-specific phosphoenolpyruvate-dependent phosphotransferase system of *Enterococcus faecalis*: Molecular cloning and nucleotide sequences of the enzyme III^{mtl} gene and the mannitol-1-phosphate dehydrogenase gene, expression in *Escherichia coli* and comparison of the gene products with similar enzymes. *J Bacteriol 173*:3709–3715.

Fleischmann RD, Adams MA, White O, Clayton RA, Kirkness EF, Kerlavage AR, Bult CJ, Tomb JF, Dougherty BA, Merrick JM, McKenney K, Sutton G, FitzHugh W, Fields C, Gocayne JD, Scott J, Shirley R, Liu LI, Glodek A, Kelley JM, Weidman JF, Phillips CA, Spriggs T, Hedblom E, Cotton MD, Utterback TR, Hanna MC, Nguyen DT, Saudek DM, Brandon RC, Fine LD, Fritchman JL, Fuhrmann JL, Geoghagen NSM, Gnehm CL, McDonald LA, Small KV, Fraser CM, Smith HO, Venter JC. 1995. Whole-genome random sequencing and assembly of *Haemophilus influenza* Rd. *Science 269*:496–512.

Friedrich GA. 1996. Moving beyond the genome projects. Does the future of genomics based drug discovery lie with the mouse? *Nat Biotechnol 14*:1234–1237.

Geerse RH, Izzo F, Postma PW. 1989. The PEP: Fructose phosphotransferase system in *Salmonella typhimurium*: FPr combines enzyme III^{Fru} and pseudo-HPr activities. *Mol Gen Genet 216*:517–525.

Henstra SA, Tolner B, Duurkens RHT, Konings WN, Robillard GT. 1996. Cloning, expression, and isolation of the mannitol transport protein from the thermophilic bacterium *Bacillus stearothermophilus*. *J Bacteriol 178*:5586–5591.

Honeyman AL, Curtiss RI. 1992. Isolation, characterization, and nucleotide sequence of the *Streptococcus mutans* mannitol-phosphate dehydrogenase gene and the mannitol-specific factor III gene of the phosphoenolpyruvate phosphotransferase system. *Infect Immun 60*:3369–3375.

Inouye S, Yamada M, Nakazawa A, Nakazawa T. 1989. Cloning and sequence analysis of the *ntrA* (*rpoN*) gene of *Pseudomonas putida*. *Gene 85*:145–152.

Jones TA, Zou J-Y, Cowan SW, Kjelgaard M. 1991. Improved methods for building protein models in electron density maps and the location of errors in these models. *Acta Cryst A47*:110–119.

Kabsch W, Sander C. 1983. Dictionary of protein secondary structure: Pattern recognition of hydrogen-bonded and geometrical features. *Biopolymers 22*:2577–2637.

Laskowski RA, MacArthur MW, Moss DS, Thornton JM. 1993. PROCHECK: A program to check the stereochemical quality of protein structures. *J Appl Cryst 26*:283–291.

Lee CA, Saier MH Jr. 1983. Mannitol-specific enzyme II of the bacterial phosphotransferase system. III. The nucleotide sequence of the permease gene. *J Biol Chem 258*:10761–10767.

Lengeler JW, Jahreis K, Wehmeier UF. 1994. Enzymes II of the phosphoenolpyruvate-dependent phosphotransferase systems: Their structure and function in carbohydrate transport. *Biochim Biophys Acta 1188*:1–28.

Lolkema JS, Ten Hoeve-Duurkens RH, Swaving-Dijkstra D, Robillard GT. 1991. Mechanistic coupling of transport and phosphorylation activity by enzyme II^{mtl} of the *Escherichia coli* phosphoenolpyruvate-dependent phosphotransferase system. *Biochemistry 30*:6716–6721.

Lux R, Jahreis K, Bettenbrock K, Parkinson JS, Lengeler JW. 1995. Coupling the phosphotransferase system and the methyl-accepting chemotaxis protein-dependent chemotaxis signaling pathways of *Escherichia coli*. *Proc Natl Acad Sci USA 92*:11583–11587.

Merrick MJ. 1993. In a class of its own—The RNA polymerase sigma factor σ^{54} (σ^{N}). *Mol Microbiol 10*:903–909.

Merrick MJ, Coppard JR. 1989. Mutations in genes downsteam of the *rpoN* gene (encoding σ^{54}) of *Klebsiella pneumonia* affect expression from σ^{54}-dependent promotors. *Mol Microbiol 3*:1765–1775.

Merrick MJ, Taylor M, Saier MH Jr, Reizer J. 1995. The role of the genes downstream of the σ^{N} structural gene *rpoN* in *Klebsiella pneumonia*. Nitrogen fixation: Fundamentals and applications. St. Petersburg, Russia: Kluwer Academic Publishers. pp 189–194.

Pelton JG, Torchia DA, Remington SJ, Murphy KP, Meadow ND, Roseman S. 1996. Structures of active site histidine mutants of III^{Glc}, a major signal-

transducing protein in *Escherichia coli*—Effects on the mechanism of regulation and phosphoryl transfer. *J Biol Chem 271*:33446–33456.

Postma PW, Lengeler JW, Jacobson GR. 1993. Phosphoenolpyruvate-carbohydrate phosphotransferase systems of bacteria. *Microbiol Rev 57*:543–594.

Powell BS, Court DL, Inada T, Nakamura Y, Michotey V, Cui XW, Reizer A, Saier MH Jr, Reizer J. 1995. Novel proteins of the phosphotransferase system encoded within the *rpoN* operon of *Escherichia coli*. Enzyme IIA^{Ntr} affects growth on organic nitrogen and the conditional lethality of an *era*^{ts} mutant. *J Biol Chem 270*:4822–4839.

Reizer J, Reizer A, Kornberg HL, Saier MH Jr. 1994. Sequence of the *fruB* gene of *Escherichia coli* encoding the diphosphoryl transfer protein (DTP) of the phosphoenolpyruvate:sugar phosphotransferase system. *FEMS Microbiol Lett 118*:159–162.

Reizer J, Reizer A, Saier MH Jr, Jacobson GR. 1992. A proposed link between nitrogen and carbon metabolism involving protein phosphorylation in bacteria. *Protein Sci 1*:722–726.

Saier MH Jr, Reizer J. 1994. The bacterial phosphotransferase system: New frontiers thirty years later. *Mol Microbiol 13*:755–764.

van Montfort RLM, Pijning T, Kalk KH, Hangyi I, Kouwijzer MLCE, Robillard GT, Dijkstra BW. 1998. The structure of the *Escherichia coli* phosphotransferase IIA^{mannitol} reveals two distinct conformations of the active site. *Structure 6*:377–388.

van Weeghel RP, Meyer GH, Keck W, Robillard GT. 1991. Phosphoenolpyruvate-dependent mannitol phosphotransferase system of *Escherichia coli*: Overexpression, purification, and characterization of the enzymatically active C-terminal domain of enzyme II^{mtl} equivalent to enzyme III^{mtl}. *Biochemistry 30*:1774–1779.

Wu LF, Tomich JM, Saier MH Jr. 1990. Structure and evolution of a multidomain multiphosphoryl transfer protein. Nucleotide sequence of the *fruB(HI)* gene in *Rhodobacter capsulatus* and comparisons with homologous genes from other organisms. *J Mol Biol 213*:687–703.